High-order harmonic generation at a repetition rate of 100 kHz

F. Lindner,[1,*] W. Stremme,[1] M. G. Schätzel,[1] F. Grasbon,[1] G. G. Paulus,[1,2] H. Walther,[1,2] R. Hartmann,[3] and L. Strüder[3]
[1]*Max Planck Institut für Quantenoptik, Hans-Kopfermann-Strasse 1, 85748 Garching, Germany*
[2]*Ludwig-Maximilians-Universität München, Am Coulombwall 1, 85748 Garching, Germany*
[3]*Max Planck Institut für extraterrestrische Physik, Halbleiterlabor, Otto-Hahn-Ring 6, 81739 München, Germany*
(Received 25 February 2003; published 18 July 2003)

We report high-order harmonic generation (HHG) in rare gases using a femtosecond laser system with a very high repetition rate (100 kHz) and low pulse energy (7 μJ). To our knowledge, this is the highest repetition rate reported to date for HHG. The tight focusing geometry required to reach sufficiently high intensities implies low efficiency of the process. Harmonics up to the 45th order are nevertheless generated and detected. We show evidence of clear separation and selection of quantum trajectories by moving the gas jet with respect to the focus, in agreement with the theoretical predictions of the semiclassical model of HHG.

DOI: 10.1103/PhysRevA.68.013814 PACS number(s): 42.65.Ky

I. INTRODUCTION

When a short, intense laser pulse interacts with an atomic gas, the atoms respond in a nonlinear way and emit efficiently coherent radiation at frequencies that are odd multiples of the laser frequency [1,2]. In recent years this phenomenon of high-order harmonic generation (HHG) has become one of the major topics in multiphoton physics, since it provides a unique source of high-brightness coherent radiation extending to the vacuum ultraviolet (VUV) and soft x-ray spectral ranges. Applications of such light sources are naturally in the fields of spectroscopy and holography. Furthermore, harmonics extending into the ''water window'' (4.4–2.3 nm) have been generated by means of tabletop laser systems [3,4], opening the way to applications in photobiology. A high repetition rate is especially desirable in the field of metrology, for coincidence experiments, and also in situations where space charge effects play a critical role.

A full understanding of the physical process can increase the flexibility of these sources in terms of spectral characteristics and tunability [5], and is therefore essential for future applications in many fields of physics. Furthermore, the effort towards increased conversion efficiencies has recently become one of the main issues in HHG [6–11]. In this respect, a thorough comprehension of the physics involved is a necessary step in the search for new solutions. For a recent review of HHG see Ref. [12].

This paper presents experimental results of HHG obtained by means of a femtosecond laser system with very high repetition rate (100 kHz). This is orders of magnitude higher than what has been reported to date for HHG. It should be pointed out that the conditions of our experiment are indeed different from those normally reported for HHG, where energies in the μJ range can be reached in the harmonics comb itself [10], whereas we use 7 μJ pulses to *generate* the harmonics. In fact, to our knowledge, this is the first experimental study of HHG at this relatively low pulse energy. Nevertheless, the conventional theoretical treatment of HHG is highly applicable and provides a simple tool for interpreting experimental results.

The paper is organized as follows. In Sec. II we recall the basic semiclassical theory of HHG and show how this model can be used to take into account single-atom response as well as phase-matching effects. In Sec. III we introduce the experimental setup, including the laser system and the extreme ultraviolet (XUV) spectrometer. In Sec. IV phase-matching effects are shown to dominate the macroscopic response of the medium, in agreement with theoretical predictions. In particular, it is shown that the position of the gas jet with respect to the laser focus can select a single ''quantum trajectory'' followed by the electron [13].

II. QUASICLASSICAL TREATMENT

A breakthrough in the theoretical framework is represented by the so-called three-step model [14,15]. According to it, the physical process of HHG can be regarded as consisting of three sequential steps. First, ionization occurs by tunneling of the electron through the potential barrier created by the atomic potential perturbed by the intense laser field. Then (second step) the dynamics of the free electron is classically governed by the oscillating laser field. The electron, therefore, follows a trajectory that strongly depends on the intensity and phase of the laser at the moment of tunneling. For linear polarization the electron may revisit the ion core, and recombination can take place (third step), giving rise to a photon with an energy equal to the instantaneous kinetic energy of the ''returning'' electron plus the ionization potential of the atom.

This description clearly indicates the role of the laser field amplitude and phase in determining the evolutions of the electron trajectory and subsequent photon emission. Since the approach is classical, the solution simply consists in solving the equation of motion of a free electron in an oscillating electric field. In the following, we consider a linearly polarized periodic field:

$$E = E_0 \sin(\omega t), \tag{1}$$

where ω is the laser's angular frequency. The electron is assumed to be shifted into the continuum with zero velocity

*Electronic address: fal@mpq.mpg.de-

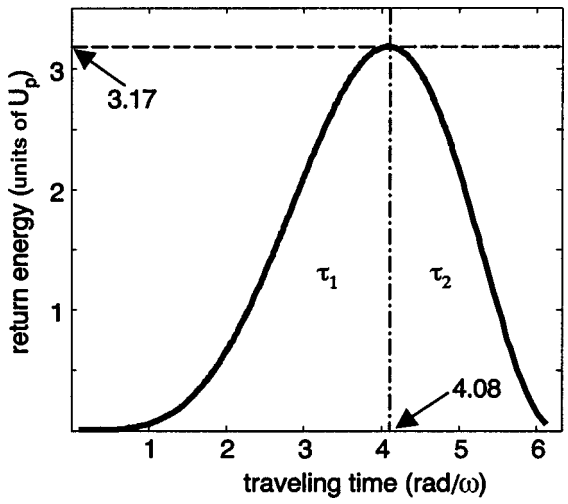

FIG. 1. Calculated kinetic energy of the electron revisiting the ion core as a function of the traveling time τ. U_p = ponderomotive energy of the laser, ω = angular frequency of the laser, τ_1 = "short" trajectories, τ_2 = "long" trajectories.

at some phase ωt_0 of the external laser field. The evolution of the electron can easily be determined from Eq. (1). Particularly, interesting for HHG is the time t_1 when the electron revisits the ion. An elegant graphical solution for determining it has been proposed [16]. Introducing the so-called "traveling time" $\tau = t_1 - t_0$, i.e., the time interval spent by the electron in the continuum, also provides an analytical solution:

$$t_0 = \frac{1}{\omega} \arctan\left(\frac{-\omega\tau + \sin\omega\tau}{1 - \cos\omega\tau} \right), \tag{2}$$

from which all parameters of interest (return time t_1 and corresponding kinetic energy) can be found.

The main results of this approach are summarized in Fig. 1, showing the instantaneous kinetic energy of the returning electron (in units of the ponderomotive energy U_p of the laser, i.e., the mean kinetic energy acquired by the electron during a cycle of the field, $U_p \propto E^2$) as a function of the traveling time (in units of phase of the laser field). The calculation predicts a maximum of $3.17U_p$ for the kinetic energy of the returning electron. This happens if tunneling occurs at a field phase of 1.88 rad, with a correspondent traveling time of 4.08 rad/ω. The subsequent maximum photon energy is given by $3.17U_p + I_p$, where I_p is the ionization potential of the atom. A sharp cutoff in the harmonic spectrum has been predicted [17] and observed [18], validating this simple physical model.

For energies lower than the cutoff, two different solutions exist. Since they differ in the traveling time, they are referred to as short (τ_1) and long (τ_2) trajectories. In particular, trajectories that started earlier (laser field phase at tunneling <1.88 rad) will return later. The picture suggests similarities to a classical projectile motion, the launch angle to the vertical being replaced by the phase of the electric field.

The fact that the harmonic emission shows peaks at odd multiples of the fundamental frequency is due to parity conservation in centrosymmetric media (typically rare gases). Similarly, the periodicity of the electric field shows that even orders, as well as arbitrarily generated frequencies, do not add in phase from cycle to cycle. They are thus rapidly washed out, whereas odd orders grow up from cycle to cycle and give a nonzero net contribution.

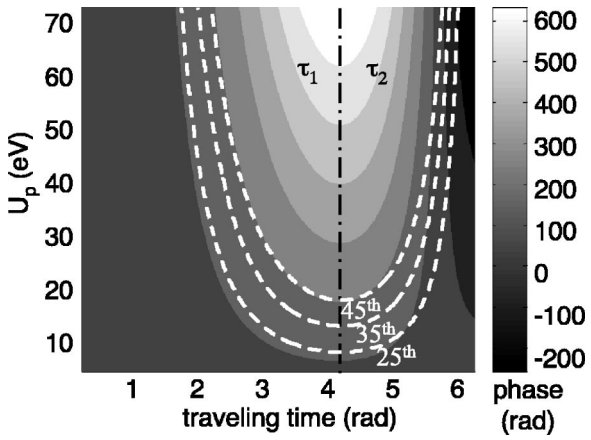

FIG. 2. Contour plot of the phase of the emitted harmonic field in argon as a function of the traveling time τ and laser ponderomotive energy U_p. The dashed lines represent the 25th, 35th, and 45th harmonics.

A fully quantum mechanical model [19] confirms the validity of the results listed above, indicating that only a few relevant quantum trajectories actually contribute to the harmonic emission. In addition, this model emphasizes the role of the phase of the emitted harmonic electric field. Indeed, since a large number of atoms are involved, the macroscopic response of the medium critically depends on the relative phases of the elementary electric fields.

According to the quantum model [20] and in the spirit of Feynman's path integral method, the radiation is emitted with a phase with respect to the fundamental proportional to the so-called quasiclassical action acquired by the electron along the trajectory followed:

$$S(p, t_0, t_1) = \int_{t_0}^{t_1} dt \left(\frac{p^2(t)}{2m_e} + I_p \right), \tag{3}$$

where t_0 is the tunneling time, t_1 the recombination time, p the electron's classical momentum, m_e the electron mass, and I_p the ionization potential of the atom. Since recombinations take place at different times t_1, all phases must be referred to a common time axis. The phase of the emitted elementary harmonic field then reads

$$\theta = -\frac{S(p, t_0, t_1)}{\hbar} + q\omega t_1, \tag{4}$$

where q stands for the harmonic order and ω stands for the laser's angular frequency.

By solving the equation of motion it is possible to calculate the above integral for all possible times t_0. Since the focusing of the laser beam in the experiments causes strong spatial variation of the intensity, it is particularly interesting to investigate the dependence of the phase of the emitted harmonics on the intensity.

Figure 2 shows a contour plot of the phase θ as a function

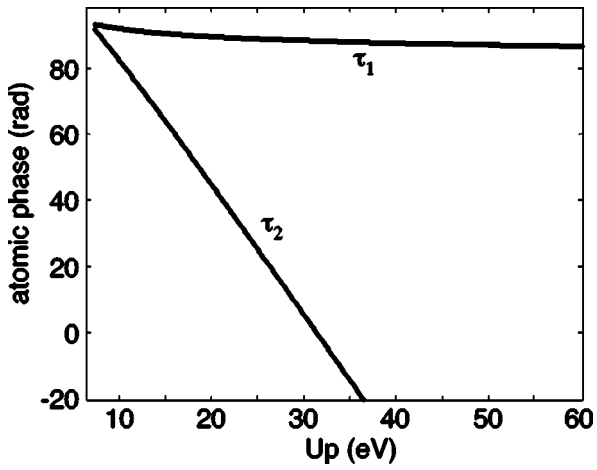

FIG. 3. Intensity dependence of the 25th harmonic in argon for the short (τ_1) and long (τ_2) trajectories.

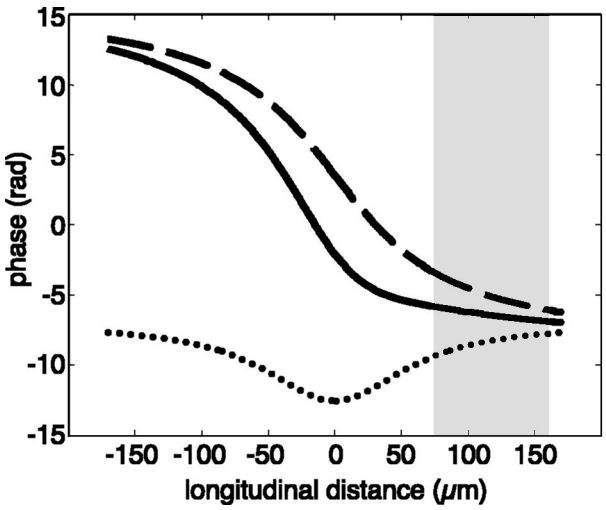

FIG. 4. Phase-matching plot on axis for the 11th harmonic (short trajectory) in argon. The laser parameters are as indicated in Sec. III. The dashed, dotted, and solid lines represent the geometrical, atomic, and resulting phases, respectively. The shading represents the area of ''good'' phase matching.

of the laser ponderomotive energy U_p and the traveling time τ. The atomic gas is argon and the fundamental wavelength is 800 nm. The dashed line connects all points giving rise to a harmonic photon of equal energy (e.g., 39 eV in Fig. 2, corresponding to the 25th harmonic). Short trajectories (τ_1, left-hand side of the plot) are characterized by small variation of the phase along the line, whereas long trajectories (τ_2, right-hand side of the plot) undergo appreciable variation of the phase. The dependence is found to be almost linear:

$$\theta = -\eta U_p, \tag{5}$$

and the coefficient η depends strongly on the type of trajectory followed (τ_1 or τ_2) and only slightly on the harmonic order and ionization potential of the atoms. For instance, for the 25th harmonic of Fig. 2 we find phases of $\theta_2 = -3.9U_p$ rad/eV and $\theta_1 = -0.11U_p$ rad/eV for the long and short trajectories, respectively. In fact, the linear approximation is very good for the former, but a bit rough for the latter, as can be seen in Fig. 3. Moreover, these values also depend on the harmonic order. In particular, harmonics generated by long trajectories are characterized by a slope slightly decreasing with increasing harmonic order, while the opposite applies to short trajectories.

Besides this intrinsic intensity-dependent ''atomic'' phase, one has to take into account the phase induced by the fundamental laser beam, known as the ''Gouy'' phase [21]. This depends on the focusing geometry only, and produces a phase shift (on axis) of $q\pi$ while passing through the focus. Incidentally, this behavior could explain the observed [22] reduction of the plateau extent, as compared with the prediction of the single-atom response. This can be understood by observing that good phase matching requires that the phase variation induced by the atomic phase be compensated by the geometrical Gouy phase. Figure 4 shows the sum of these two phases (on axis) for the case of the short trajectory and for a low-order harmonic (11th), indicating that this compensation selects an area of ''good'' phase matching. Since only the geometrical phase scales with the harmonic order q, depending on the laser parameters phase matching will eventually degrade with increasing harmonic order, thus leading to a reduced plateau extent.

For the sake of completeness, one should also consider dispersion effects due to neutral atoms, ions, and, in particular, free electrons. However, since in our experiments we deal with low pressures (<10 mbar) and very tight focusing geometry (f-number 8), none of these effects play a crucial role. Even in the (nonrealistic) case of complete ionization of the atomic medium, the coherence length (i.e., the length over which the phase slippage is π) associated with the dispersion of the free electrons is of the order of the laser confocal parameter. In this range, the variation of the Gouy phase is much larger. Hence, all dispersion effects will be neglected.

One might argue that the atomic phase does not produce a large phase variation through the focus compared with the Gouy phase either, and that one could also neglect it. Note, however, that both the Gouy phase and free electron dispersion phase have odd symmetry around the focus, while the atomic phase has even symmetry, being proportional to the intensity. Neglecting it would thus qualitatively change the physical picture, while neglecting the free electron phase only results in a (good) numerical approximation. This observation is also supported by the experimental results (see Sec. IV) that clearly indicate the balancing of two-phase contributions of different symmetry.

Figure 5 shows contour plots of the phase of the 25th harmonic generated in argon. It results from the sum of the intrinsic atomic phase and the geometrical phase, including the Gouy phase and the curvature of the laser phase front. The laser parameters correspond to those used in our experiments (see Sec. III). The beam propagates from left to right, and the radial symmetry is guaranteed. Note that, according to the model, the diagrams have physical meaning only inside the solid line, where the intensity is high enough to

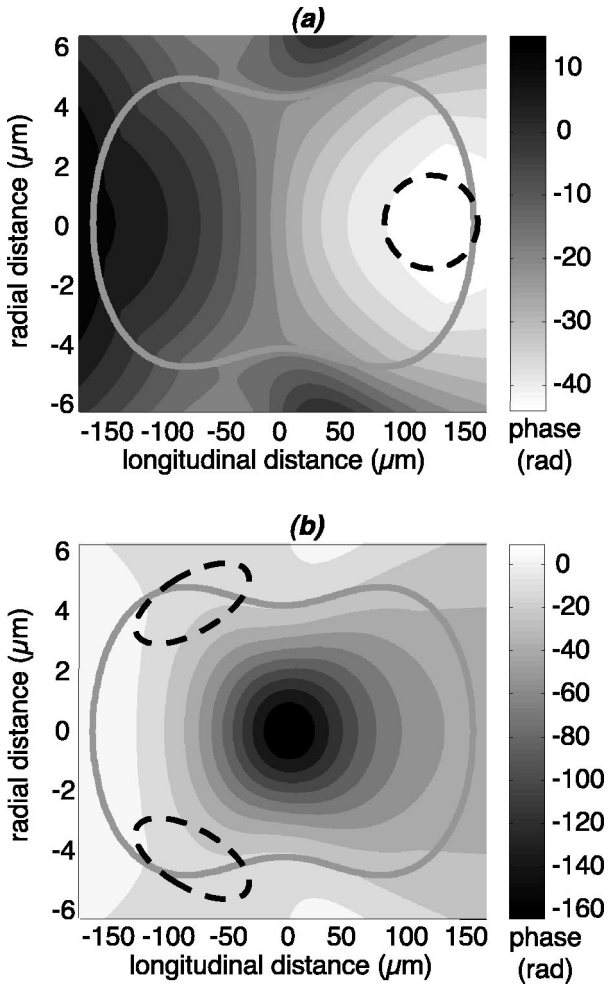

FIG. 5. Contour map of the phase of the 25th harmonic in argon for the short (a) and long (b) trajectories. The laser parameters are as indicated in Sec. III. The solid lines represent the cutoff intensity for the 25th harmonic; the dashed lines indicate areas of "good" phase matching.

create the harmonic considered. The harmonic field can efficiently develop only if phases during generation match over a significant area. For the sake of clarity, the phase accumulated by the propagation of a plane wave in the forward direction ($-qkz$) has already been subtracted. Constructive interference in the forward direction therefore occurs where the displayed phases have the same value, i.e., where the gradient approaches zero (dashed-line regions in Fig. 5).

A striking difference appears in phase-matching conditions for short [Fig. 5(a)] and long [Fig. 5(b)] trajectories. The latter gives rise to a rapidly varying phase, with only a small off-axis annular region of good phase matching before the focus [23]. On the other hand, short-trajectory-generated harmonics show a quite flat phase, with a large on-axis region of very good phase matching after the focus. This behavior has been pointed out in the previous works [24,25] and can be reproduced fairly well by means of the semiclassical model. These remarkable differences should be recognizable in the experimental results.

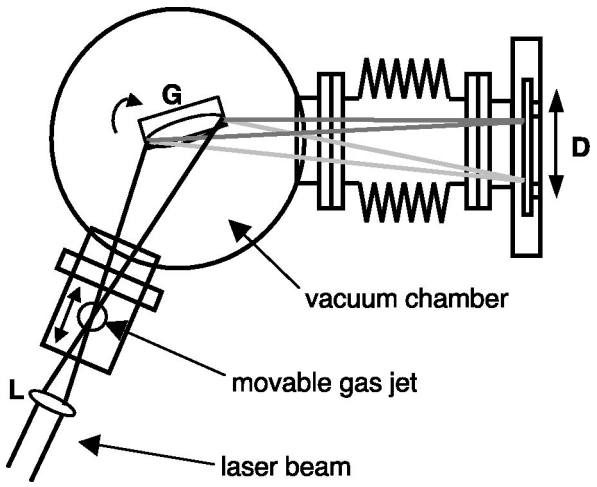

FIG. 6. The XUV spectrometer for high-order harmonic detection. L, achromatic lens ($f=80$ mm); *G*, flat-field toroidal grating; *D*, pn-CCD detector.

III. EXPERIMENTAL SETUP

The laser system [26] used in our experiments is an 800-nm Ti:sapphire regenerative amplifier system delivering pulses of 7 μJ at a repetition rate of 100 kHz. It consists of a femtosecond oscillator, a regenerative amplifier, a prism compressor and a spatial light modulator in a $4f$ setup for fine dispersion compensation. The pulse duration is 35 fs full width at half maximum.

The relatively low pulse energy requires a tight focusing geometry in order to reach the high intensities necessary for driving the nonlinear process. The beam is expanded and focused (f-number 8) with an achromatic lens ($f=80$ mm, B. Halle Nachfl., Berlin) into a rare gas jet. Intensities of up to 3×10^{14} W/cm^2 are reached in the focus ($U_p=18$ eV). However, since the interaction volume is extremely small (confocal parameter ≈100 μm), the conversion efficiency into the harmonics comb is $<10^{-9}$, i.e., lower than normally reported in HHG experiments. The detection of the light field has, therefore, to be optimized. Advantage can be taken of the very high repetition rate of the laser. However, also high efficiency of the XUV spectrometer is essential. This is schematically illustrated in Fig. 6.

The gas pressure before the effusive nozzle (diameter $=100$ μm) is usually kept between 100 and 300 mbar. The nozzle position can be finely adjusted in all directions. On the basis of gas flow measurements, we estimated a pressure in the interaction volume not exceeding 5–10 mbar. Note that at these low pressures the absorption length ($L_{abs}=1/\sigma\rho$, where ρ is the gas density and σ is the ionization cross section [27]) for, for example, the 25th harmonic generated in argon is a few millimeters, i.e., much larger than the medium length. In this particular focusing geometry, reabsorption, therefore, does not play any role.

The generating gases used in our experiments are typically argon, krypton, and xenon. Due to the lower ionization potential, the latter is characterized by a higher yield and a less pronounced plateau extension. However, no qualitative differences have been observed with respect to quantum tra-

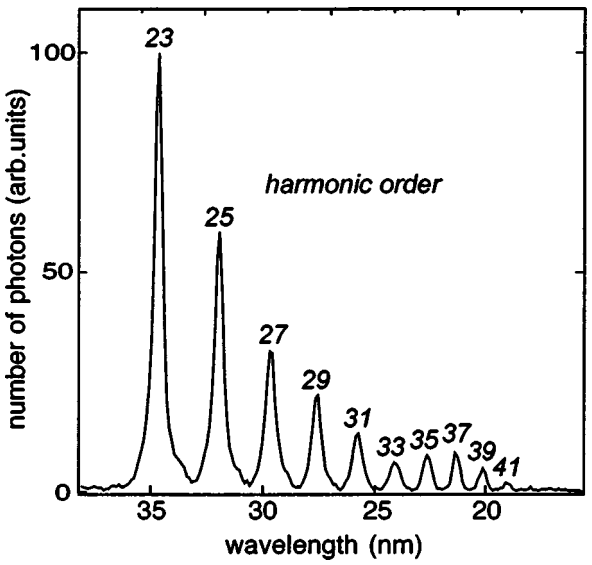

FIG. 7. Typical harmonic spectrum detected with the XUV spectrometer.

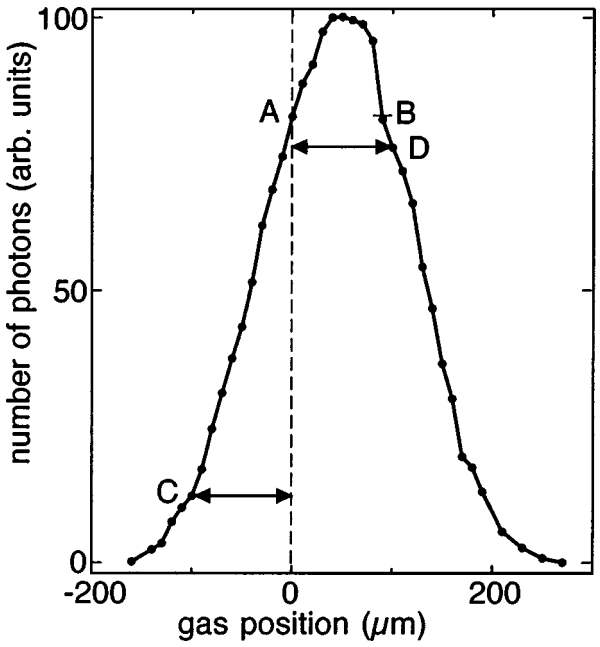

FIG. 8. Conversion efficiency (arb. units) for the 25th harmonic in argon as a function of the position of the gas jet. The laser parameters are as indicated in Sec. III.

jectory separations. For this reason, most systematic studies were carried out with argon (see Sec. IV).

The high-order harmonics generated are incident on a flat-field toroidal grating (1800 grooves/mm, Jobin-Yvon Instruments, S.A.) that separates and focuses the harmonics. A thin (2000 Å) aluminum filter in front of the detector removes scattered light from the fundamental beam. The detector is placed in the focal plane at a distance of approximately 40 cm from the grating. It consists of a backside illuminated pn–charged coupled device (CCD) chip [28,29] of very high quantum efficiency (20–70 %) in the range 15–70 eV. The detector length is 30 mm (64×200 pixels), which yields a spectral resolution of approximately 1 Å/pixel. Figure 7 shows a typical harmonics spectrum.

IV. TRAJECTORY SEPARATION

In Sec. II the different behaviors of phase-matching conditions with respect to the electron trajectory were pointed out. In particular, the optimum occurs in a region located after the focus, and short trajectories τ_1 are favored. Figure 8 shows the measured conversion efficiency into the 25th harmonic as a function of the nozzle position with respect to the focus. The generating gas is argon. Although the gas jet size is comparable to the focus size in our experiments, testing of the position dependence of phase matching is still possible owing to the density profile of the gas.

The maximum conversion efficiency occurs approximately 100 μm after the focus, indicating, in agreement with the theoretical analysis, that the short trajectory dominates [see Fig. 5]. Note that other effects producing asymmetries, such as reabsorption in the atomic gas, would lead to a maximum on the opposite side of the focus. Hence, what is observed is clearly a phase-matching effect. The observed asymmetry also indicates, as already outlined in Sec. II, that phase terms of different symmetry (i.e., the Gouy and atomic phases) compensate each other.

The phase modulation induced by the atomic response discussed in Sec. II has interesting consequences on the spectral characteristics of the high-order harmonics generated [12]. Since we are dealing with short pulses and high peak intensities, the rapid time variation of the intensity results in modulation of the instantaneous harmonic frequency:

$$\delta\omega = -\frac{\partial\theta}{\partial t} = +\eta\frac{\partial I}{\partial t}, \tag{6}$$

and therefore in broadening of the spectrum. In particular, the leading edge of the harmonic pulse is blue shifted, and the trailing edge is red shifted. In other words, the generated harmonic carries a negative chirp that depends on the peak intensity, the pulse duration, and the slope (η) of the atomic phase. This phenomenon is similar to self-phase modulation of an intense laser pulse in a medium with negative Kerr index n_2 [30]. A measurement of this induced chirp on high harmonics was recently proposed [31].

The maximum broadening should be observed at the laser focus, where the temporal derivative of I is largest. Figure 9(a) shows the spectrum of the 25th harmonic for two different positions of the gas jet (A and B in Fig. 8). For both positions the conversion efficiency (represented by the integral of the harmonic peak) is the same, i.e., the number of photons generated is equal. As expected, when the gas jet is located exactly in the focus (case A), the larger phase modulation experienced results in a broader peak than in case B, where the peak intensity is lower.

More interestingly, we can compare the spectra corresponding to two symmetric positions of the nozzle with respect to the focus [Fig. 9(b), corresponding to positions C and D in Fig. 8]. The peak intensity of the fundamental is now the same in the two cases, and differences in the spectra

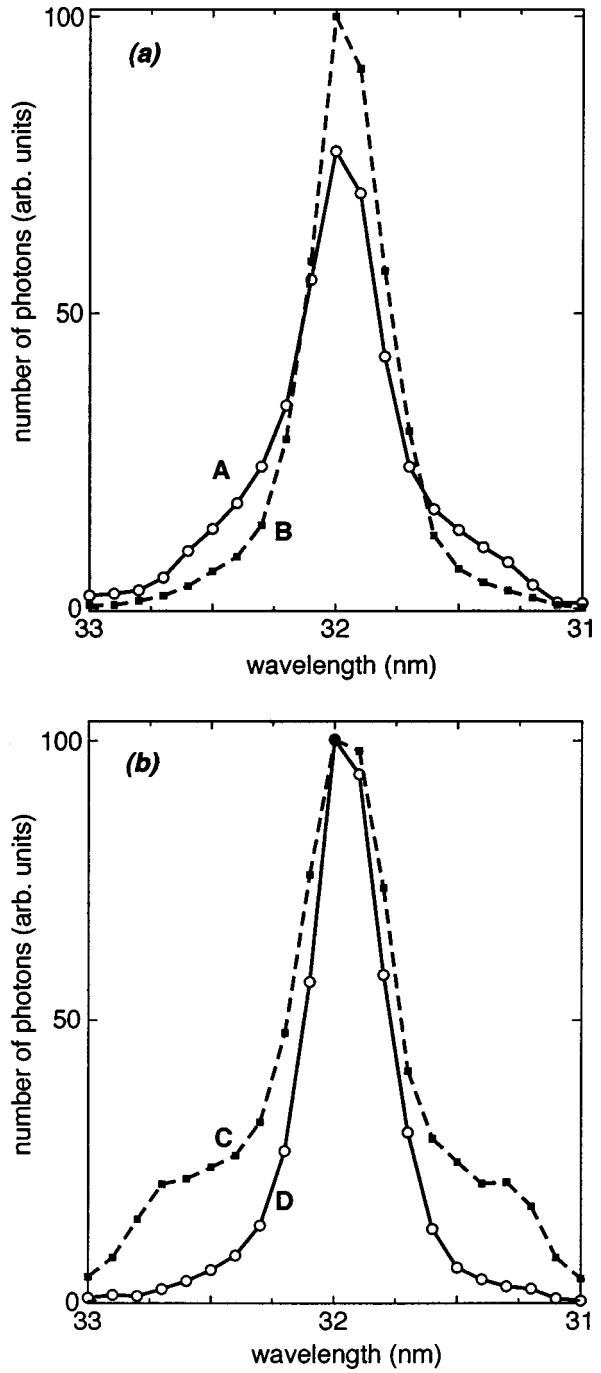

FIG. 9. Spectrum of the 25th harmonic peak for various positions of the gas jet (*A*, *B*, *C*, *D* of Fig. 8). (a) Influence of the peak intensity on the spectral broadening. The conversion efficiency (represented by the integral of the spectrum) in *A* and *B* is identical. (b) Influence of the electron trajectory on the spectral broadening. Since the conversion efficiency in *C* is lower than that in *D*, suitable normalization is necessary for the sake of clarity.

must be explained in terms of the coefficient η in Eq. (6). The peak observed in *D* is relatively narrow, while in *C* it is broader and suggests a double structure. Indeed, the position *C* corresponds [see Fig. 5] to a region where the harmonics can be efficiently generated off axis from the electrons that have followed the long (τ_2) trajectory. In fact, the spectrum in *C* may actually consist of two superimposed contributions, one from the short trajectory (with phase matching almost degraded), giving rise to the central peak, and the other from the long trajectory (with increasingly good phase matching), leading to the observed wings in the spectrum. The harmonic pulse would thus be characterized by different generation processes, and therefore by regions of different spatial and temporal coherence [32,33].

The chirp of the harmonics induced by the rapid phase variation can, in principle, be controlled by an appropriate chirp on the fundamental laser pulse. If the fundamental beam carries a positive chirp, the ''red'' frequencies on the leading edge of the pulse will be blue shifted, and the ''blue'' frequencies on the trailing edge will be red shifted. The resulting spectrum will thus appear quite narrow and will be limited by the natural bandwidth of the harmonic pulse. On the other hand, for a negative chirp on the fundamental one should observe enhanced spectral broadening. This has been pointed out both theoretically [34] and experimentally [35,36]. However, these experiments were conducted under conditions where ionization plays a major role, resulting in strong blue shifting or red shifting of the harmonic radiation.

Numerical estimates similar to that presented in Ref. [33] show that, at least for orders where a clear separation between short and long trajectories is possible, i.e., not too close to the cutoff, this control is only possible for harmonics generated with the short trajectory. Indeed, the phase variation corresponding to the long trajectory is so large that the correspondent chirp determines in any case the observed spectral width. This is not true of the τ_1 contribution, characterized by a slower phase variation (see Fig. 3), for which chirp compensation is feasible.

By locating the gas jet in a position where the short trajectory dominates, we analyzed the spectra of the harmonic peaks as a function of the chirp of the fundamental. This can easily be changed by adjusting the voltages of the spatial light modulator used in the laser system [26]. Figure 10 shows the spectra of the 27th harmonic in argon for positive, negative, and zero chirp applied. These are purely quadratic and correspond approximately to $+200$ fs^2, -200 fs^2 (corresponding to a pulse duration of 40 fs), and 0 fs^2 (35 fs). Since the pulses become longer when they carry a residual chirp, the conversion efficiency (represented by the integral of the harmonic spectrum) is higher in the case of no chirp. Note that no relevant blue or red shifting of the harmonic peak can be observed, indicating that ionization is not a major effect in our experiments.

The narrow peak and the enhanced broadening observed for application of positive and negative chirp, respectively, confirm the agreement between the theoretical analysis and the experimental data. In particular, the macroscopic separation into the two quantum trajectories is here once more corroborated. Furthermore, this last result traces an extremely simple way of tailoring the shape of the spectrum on demand, a feature that might be essential for future applications of high harmonics.

V. CONCLUSION

We have presented experimental results obtained under conditions different from those normally reported for HHG.

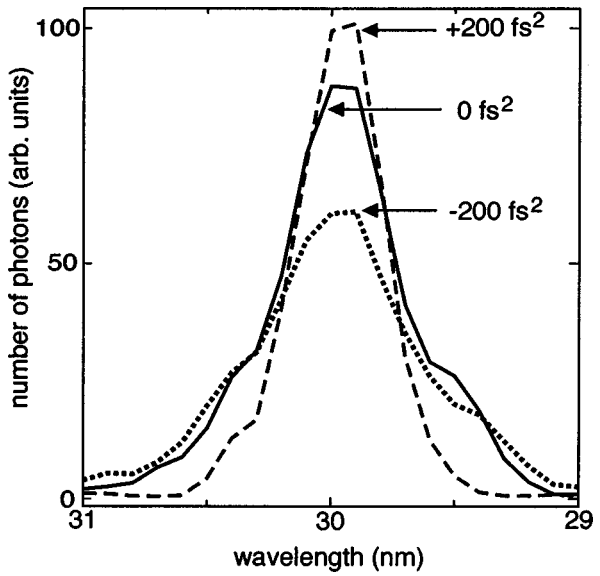

FIG. 10. Spectrum of the 27th harmonic peak for positive (dashed line), negative (dotted line), and zero (solid line) chirp of the fundamental beam.

To our knowledge, this is the first experimental study of high-order harmonics performed at very high repetition rate (100 kHz). The low pulse energy requires extremely tight focusing geometry, normally not used in HHG for the consequent low conversion efficiency. Under these conditions, free electrons due to ionization do not play a crucial role and phase matching is entirely determined by the atomic and geometrical phases.

Despite these differences with normal HHG setups, we have shown that the semiclassical treatment of the physical process is essentially valid and represents a simple method of intuitively modeling the single-atom response and predicting the macroscopic response of the atomic media. We identified clear evidence of phase-matching effects and, in particular, of separation of quantum trajectories by adjusting the gas position. This effect, predicted [33] and observed [13], is here confirmed under qualitatively different experimental conditions.

It should be noted that not only is separation of the harmonic field into the two τ_1 and τ_2 components a significant result from the point of view of theoretically understanding the HHG process, it can also represent a way of providing xuv radiation with desired spatial and spectral characteristics. In this respect, adjusting the laser fundamental chirp seems to be an efficient way of shaping the spectrum of the harmonics and hence their coherence properties.

ACKNOWLEDGMENTS

We would like to thank R. Stötter and C. von Zanthier for technical support with the CCD detector, F. Zacher for the initial design of the experiment, and P. Salières for fruitful discussions of the physics.

[1] M. Ferray, A. L'Huillier, X.F. Li, L.A. Lompré, G. Mainfray, and C. Manus, J. Phys. B **21**, L31 (1988).

[2] A. McPherson, G. Gibson, H. Jara, U. Johann, T.S. Luk, I.A. McIntyre, K. Boyer, and C.K. Rhodes, J. Opt. Soc. Am. B **4**, 595 (1987).

[3] C. Spielmann, N.H. Burnett, S. Sartania, R. Koppitisch, M. Schnürer, C. Kan, M. Lenzner, P. Wobrauschek, and F. Krausz, Science **278**, 661 (1997).

[4] Z. Chang, A. Rundquist, H. Wang, M.M. Murnane, and H.C. Kapteyn, Phys. Rev. Lett. **79**, 2967 (1997).

[5] C. Altucci, R. Bruzzese, C. de Lisio, M. Nisoli, S. Stagira, S. De Silvestri, O. Svelto, A. Boscolo, P. Ceccherini, L. Poletto, G. Tondello, and P. Villoresi, Phys. Rev. A **61**, R021801 (1999).

[6] A. Rundquist, C.G. Durfee, III, Z. Chang, C. Herne, S. Backus, M.M. Murnane, and H.C. Kapteyn, Science **280**, 1412 (1998).

[7] M. Schnürer, Z. Cheng, M. Hentschel, G. Tempea, P. Kálmán, T. Brabec, and F. Krausz, Phys. Rev. Lett. **83**, 722 (1999).

[8] E. Constant, D. Garzella, P. Breger, E. Mével, Ch. Dorrer, C. Le Blanc, F. Salin, and P. Agostini, Phys. Rev. Lett. **82**, 1668 (1999).

[9] Y. Tamaki, J. Itatani, Y. Nagata, M. Obara, and K. Midorikawa, Phys. Rev. Lett. **82**, 1422 (1999).

[10] J.-F. Hergott, M. Kovacev, H. Merdji, C. Hubert, Y. Mairesse, E. Jean, P. Breger, P. Agostini, B. Carré, and P. Salières, Phys. Rev. A **66**, R021801 (2002).

[11] A. Paul, R.A. Bartels, R. Tobey, H. Green, S. Weiman, I.P. Christov, M.M. Murnane, H.C. Kapteyn, and S. Backus, Nature (London) **421**, 51 (2003).

[12] P. Salières, A. L'Huillier, P. Antoine, and M. Lewenstein, Adv. At., Mol., Opt. Phys. **41**, 83 (1999).

[13] P. Salières, B. Carré, L. Le Déroff, F. Grasbon, G.G. Paulus, H. Walther, R. Kopold, W. Becker, D.B. Milošević, A. Sanpera, and M. Lewenstein, Science **292**, 902 (2001).

[14] K.C. Kulander, K.J. Schafer, and J.L. Krause, in *Super-Intense Laser-Atom Physics*, Vol. 316 of *NATO Advanced Study Institute, Series B: Physics*, edited by B. Piraux, A. L'Huillier, and K. Rzazewski (Plenum, New York, 1993).

[15] P.B. Corkum, Phys. Rev. Lett. **71**, 1994 (1993).

[16] G.G. Paulus, W. Becker, and H. Walther, Phys. Rev. A **52**, 4043 (1995).

[17] J.L. Krause, K.J. Schafer, and K.C. Kulander, Phys. Rev. Lett. **68**, 3535 (1992).

[18] A. L'Huillier and Ph. Balcou, Phys. Rev. Lett. **70**, 774 (1993).

[19] M. Lewenstein, Ph. Balcou, M.Yu. Ivanov, A. L'Huillier, and P.B. Corkum, Phys. Rev. A **49**, 2117 (1994).

[20] M. Lewenstein, P. Salières, and A. L'Huillier, Phys. Rev. A **52**, 4747 (1995).

[21] A.E. Siegman, *Lasers* (University Science Books, Mill Valley, CA, 1986).

[22] A. L'Huillier, M. Lewenstein, P. Salières, Ph. Balcou, M.Yu. Ivanov, J. Larsson, and C.G. Wahlström, Phys. Rev. A **48**, R3433 (1993).

[23] Note that slightly better phase-matching conditions could be expected by considering local propagation in arbitrary directions (i.e., subtracting tilted waves in Fig. 5), which would yield harmonics of bigger divergence. However, the position and size of the areas of good phase matching do not significantly change for small angles.
[24] P. Salières, A. L'Huillier, and M. Lewenstein, Phys. Rev. Lett. **74**, 3776 (1995).
[25] Ph. Balcou, P. Salières, A. L'Huillier, and M. Lewenstein, Phys. Rev. A **55**, 3204 (1997).
[26] F. Lindner, G.G. Paulus, F. Grasbon, A. Dreischuh, and H. Walther, IEEE J. Quantum Electron. **38**, 1465 (2002).
[27] W.F. Chan, G. Cooper, X. Guo, G.R. Burton, and C.E. Brion, Phys. Rev. A **46**, 149 (1992).
[28] R. Hartmann, K.-H. Stephan, and L. Strüder, Nucl. Instrum. Methods Phys. Res. A **439**, 216 (2000).
[29] L. Strüder, Nucl. Instrum. Methods Phys. Res. A **454**, 73 (2000).
[30] A.E. Shen, *The Principles of Nonlinear Optics* (Wiley-Interscience, New York, 1984).
[31] T. Sekikawa, T. Katsura, S. Miura, and S. Watanabe, Phys. Rev. Lett. **88**, 193902 (2002).
[32] M. Bellini, C. Lyngå, A. Tozzi, M.B. Gaarde, T.W. Hänsch, A. L'Huillier, and C.G. Wahlström, Phys. Rev. Lett. **81**, 297 (1998).
[33] M.B. Gaarde, F. Salin, E. Constant, Ph. Balcou, K.J. Schafer, K.C. Kulander, and A. L'Huillier, Phys. Rev. A **59**, 1367 (1999).
[34] P. Salières, P. Antoine, A. de Bohan, and M. Lewenstein, Phys. Rev. Lett. **81**, 5544 (1998).
[35] J. Zhou, J. Peatross, M.M. Murnane, H.C. Kapteyn, and I. Christov, Phys. Rev. Lett. **76**, 752 (1996).
[36] Z. Chang, A. Rundquist, H. Wang, I. Christov, H.C. Kapteyn, and M.M. Murnane, Phys. Rev. A **58**, R30 (1998).